AIAA Regional Student Conferences
, Multiple Locations
2025 Regional Student Conferences

10.2514/6.2025-98452

Preliminary Design Study for a Blended Wing Body Seaplane

Nyhel Sekulic*, Theo Altneu†, Patrick Kupiec‡, Alex Higuera Pierre Noel§, Gavin Vetro¶, Eric Clark‖
University of Arizona, Tucson, Arizona, 85721, United States

This study investigates the aerodynamic characteristics of two configurations of a Blended Wing Body amphibious cargo seaplane: a baseline design and a variant equipped with catamaran-style floats. These configurations are intended for long-range offshore mission support. The goals of this project are to optimize the design to meet our performance requirements, to increase our coefficient of lift and decrease our coefficient of drag, to quantify the drag penalty introduced by the floats and to explore strategies for drag reduction and improved longitudinal stability. Experimental methods included Computational Fluid Dynamics simulations and low-speed wind tunnel testing using a force balance and 3D-printed models. Aerodynamic performance was evaluated over a range of angles of attack at constant Reynolds numbers, yielding key metrics such as lift, drag, pitching moment coefficients, and lift-to-drag ratios. The results highlight the aerodynamic penalties of the float configuration and reveal opportunities for reducing drag while enhancing lift and stability through design refinements. These findings demonstrate the feasibility of optimizing the Blended Wing Body seaplane concept for improved performance in future iterations.

I. Nomenclature

C_l	=	coefficient of lift
C_d	=	coefficient of drag
C_m	=	coefficient of pitching moment
C_j	=	jet coefficient
L/D	=	lift over drag ratio
α	=	angle of attack
W_E	=	weight empty
W_F	=	weight of fuel
W_{TO}	=	takeoff weight
W_{PL}	=	payload weight
W_{tfo}	=	weight of the trapped fuel and oil
W_{crew}	=	weight of crew
$W_{F_{used}}$	=	weight of fuel used
$W_{F_{res}}$	=	weight of fuel and reserves
V_{cr}	=	cruising velocity
$Cruise_{ff}$	=	cruising fuel fraction
M_{ff}	=	mission fuel fraction
A	=	weight regression coefficient
B	=	weight regression coefficient
C	=	weight regression coefficient
R_e	=	Reynolds number
q_∞	=	free-stream dynamic pressure

*Undergraduate Student, Department of Systems and Industrial Engineering, AIAA Student Member, 1809785.
†Undergraduate Student, Department of Aerospace and Mechanical Engineering, AIAA Student Member, 1809883.
‡Undergraduate Student, Department of Aerospace and Mechanical Engineering, AIAA Student Member, 1809880.
§Undergraduate Student, Department of Aerospace and Mechanical Engineering, AIAA Student Member, 1739841.
¶Undergraduate Student, Department of Aerospace and Mechanical Engineering, AIAA Student Member, 1809987.
‖Undergraduate Student, Department of Aerospace and Mechanical Engineering, AIAA Student Member, 1799375.

II. Introduction

BLENDED Wing Body (BWB) aircraft configurations are an innovative design concept that merges the fuselage with the wings into a seamless structure to turn the fuselage into a lifting structure. A BWB seaplane has not been conceptualized until this design study, and thus the task of analyzing and presenting the preliminary data is completely unique. All in all, this project combines the iterative nature of research and design with the analytical aspects of wind tunnel testing and computational fluid dynamics simulation to deliver the aforementioned preliminary data on lift and drag. The natural first step in creating a new aircraft is to begin with the specified requirements and utilize them to create test conditions that guide the initial sizing requirements of the aircraft. Taking all of these parameters into account provides the basis of a carpet plot. All of these steps ultimately culminate in a simple determination of the wingspan and the area of the wing platform. After the initial sizing and design is complete, the next step is to begin testing, which serves as the basis for which changes to the system will be made in order to improve performance and stability in future design iterations. Wind tunnel tests provide realistic results at the expense of time and coordination with the owners and operators of the aforementioned wind tunnel. Computational Fluid Dynamics (CFD) simulation is a form of computer simulation that allows for aerodynamic forces to be examined across a body when exposed to a flow in a fluid, in this case air, as well as their respective moments.

III. Design

A. Initial Sizing

In order to begin designing the seaplane, a weight regression model was used, based on previous BWB aircraft, with the key distinction being that they are not the same size as the BWB, nor are they amphibious. Acquiring data from this graph serves to at least develop a baseline upon which to create initial weight estimations for the BWB. The graph of previous BWB aircraft was plotted on a log-log axis system including mean takeoff weight (MTOW) versus the empty weight of each aircraft. Applying a fitted line to these data allows for the weight regression coefficients, A and B, to be observed, allowing for a point along the linear fit to be chosen that fits the trend, and thereby indicates a reasonable estimation for early BWB sizing. Figure 1. contains the weight regression plot and coefficients.

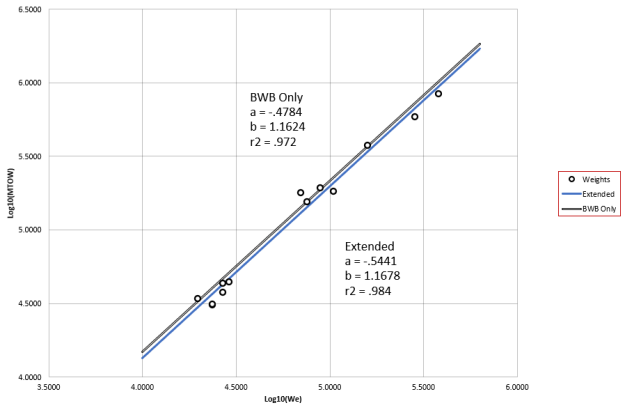

Fig. 1 Weight Regression Plot

The weight regression coefficients can then lead to the initial sizing of the BWB aircraft. Our study investigated two types of propulsion system: turboprop gas turbine engine and turbofan gas turbine engine. Each type of engine was considered to determine which allowed the aircraft to be as light as possible while providing the necessary amount of thrust to reduce weight. Engine performance parameters from [1] was used as examples to proceed with initial sizing. A general guideline for initial sizing is summarized in Equation 1.

$$W_{TO} = W_E + W_F + W_{PL} \tag{1}$$

Where

$$W_E = W_{tfo} + W_{crew} \tag{2}$$

$$W_F = W_{F_{used}} + W_{F_{res}} \tag{3}$$

Note that in order to estimate the amount of fuel used for the mission, the fuel fraction method was put into effect. Each segment of the mission profile was broken down into phases, and each phase had a determined amount of fuel used. The phases of the BWB seaplane are: engine start, taxi, take-off, climb, cruise, descent, landing taxi, and shutdown. Each phase fuel percentage used is based on Table 2.1 in [2]. However, the cruise phase utilized Brugret's range equation. The fuel fraction for the cruise phase was solved, resulting in Equation 4.

$$\text{Cruise}_{\text{ff}} = \frac{1}{\exp\left(\frac{\text{Range}}{\left(\frac{V_{\text{cr}}}{c_j}\right)\left(\frac{L}{D}\right)}\right)}. \tag{4}$$

The maximum amount of fuel needed for a range of 1000 knots is approximately 24000 lbs, where

$$W_F = \left(1 - M_{ff}\right) W_{TO} + W_{F_{\text{res}}} \tag{5}$$

Finally, using sensitivity studies, which take into account the weight regression coefficients, MTOW was determined iteratively with Equation 6.

$$W_{T0} = \left|A + B\ \log_{10}\left(C\ W_{T0} - D\right)\right| \tag{6}$$

Note that this is an implicit solution, where MTOW is initially guessed and converged upon. For cruise conditions of 300 knots, the MTOW converged at 141,000 lbs. With the known weights, size matching methods were used to provide the initial parameters of the aircraft.

B. Airfoil Selection

The NACA 4-series airfoils were selected for this aircraft due to their simplicity, reliable performance in low-speed flight, and relatively flat design. This choice is also influenced by the cargo bay layout and float integration, as high-camber airfoils would encroach on cargo space, requiring a larger fuselage and consequently increasing drag. To balance aerodynamic efficiency and cargo capacity, the airfoil camber is set at 4% with its maximum located at 40% of the chord. This configuration provides a C_l of 1.5 while maintaining a high L/D. This selection serves as the foundation for the iterative design, where refinements will be guided by CFD analysis and wind tunnel results. As a blended-wing design, the aircraft body incorporates a NACA 4421 airfoil. This selection was guided by key design requirements mentioned earlier, a minimum cargo bay dimension of 40 ft (L) x 10 ft (W) x 9 ft (H). With a thickness of 21% of the chord length, the NACA 4421 provides sufficient internal volume for the cargo. Furthermore, aerodynamic analysis determined that the airfoil must achieve a C_l of 1.5 which was calculated from aspect ratio, weight capacity, and FAA requirements for during take-off and landing distances. For the wings, the NACA 4412 airfoil was chosen. Compared to the fuselage airfoil, its thickness is reduced from 21% to 12%, decreasing drag and improving L/D. Despite the reduced thickness, the wing structure still provides adequate space for structural components and fuel storage.

Due to the large size of the cargo bay, selecting an airfoil and sizing it to ensure that the cargo bay fits is not a feasible option. This results in an over-sized airfoil with excess thickness below the cargo bay. Creating a custom airfoil to meet the stability requirements and cargo size is the best option. The airfoil must accommodate the payload compartment without an unreasonable airfoil thickness ratio. In addition, it needs to have a relatively blunt nose for the visibility requirements of the FAR cockpit. The configuration for the first design of the seaplane follows the design process as laid out in [3] and [4].

The design began with NASA SC(2)-0010 and SC(2)-0012 symmetric airfoils. However, the SC(2)-0012 lacked sufficient thickness to meet the payload compartment sizing requirement. To address this, a hybrid approach was taken by combining the upper surface 18% with the lower surface 12%. Lastly, modifying the aft of the airfoil by 60% resulted in a new custom airfoil that met all the sizing requirements, designated as CS(2)-1812 This new airfoil will be used on the second revision of the seaplane design.

Fig. 2 SC(2)-0012 Airfoil

Fig. 3 Hybrid SC(2)-0018 upper/ SC(2)-0012 lower Airfoil

Fig. 4 CS(2)-1812 Airfoil

An analysis using XFLR5 was conducted to compare the CS(2)-1812 with the NASA SC(2)-0012 and the hybrid configuration featuring the SC(2)-0018 upper surface and SC(2)-0012 lower surface.

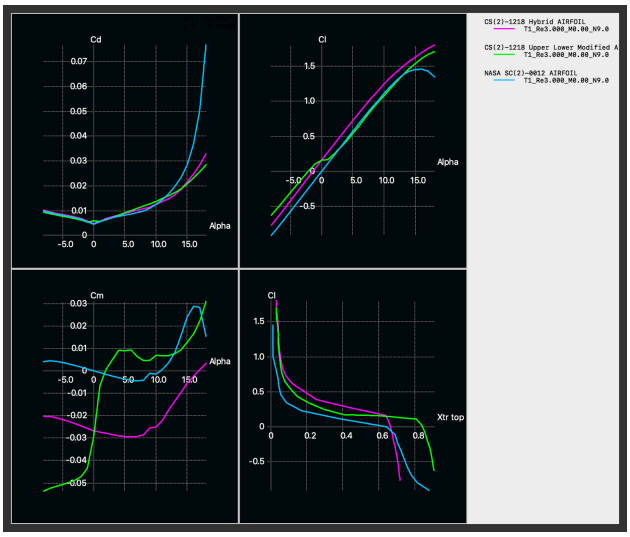

Fig. 5 Airfoil Comparison Results

Figure 5. shows that CS(2)-1812 not only outperformed in lift and drag but also displayed a relatively flat Cm curve. This new airfoil will be integrated into the second iteration design to further analyze static stability.

C. Float Selection

Three different designs of catamaran-style floats were created using proprietary design tools created by the New Nose Company with reference to [5]. The forward sections of the floats were all identical. The aft sections of the floats differed in how they terminated. In the first design (Type I), the conic control point was placed 20° from the horizontal, and the edge was truncated to a flat face. For the second design (Type II), the conic control point was put at right angle and the terminating section came to a soft, curved point. For the third design (Type III), the conic control point was again angled 20° from the horizontal and the terminating section came to a sharper point.

IV. Analysis

A. Float Drag Study

The three float designs were compared to determine which model would have the lowest overall drag contribution. Fluid simulations were carried out using SOLIDWORKS Flow Simulation, with flow conditions matching the cruising test condition, which is International Standard Atmosphere (ISA) + 15℃ at 10,000 feet and V = 300 knots. The computational domain was established such that the top face of the float was coincident with the top face of the enclosure, as the top face of the float would be modeled into the plane in the actual model. SOLIDWORKS Flow Simulation was

then run until the model converged. The force in the z-direction (drag) was recorded and a contour plot of the velocity along the plane of symmetry was produced.

B. Wind Tunnel Testing

Wind tunnel testing was carried out in the 12x12-inch open circuit University of Arizona Educational Wind Tunnel (EWT) at an approximately constant q_∞ = 14.5 kPa for an α range of -10° to 10° in 2° steps for both models. With the selected experiment conditions, $R_e = 1.05 \times 10^5$ was achieved, with boundary layer transition trips added to further increase the test R_e for both models. Despite not reaching a high Re due to the space and velocity limitations of the EWT, the expected results and their usefulness remain unchanged. The objective was to obtain C_l, C_d, C_d, and L/D plots as a function of α for the no floats and floats-equipped models for direct comparison of their aerodynamic characteristics, with a special emphasis in the C_d penalty of including floats.

C. Computational Fluid Dynamics Simulations

CFD tests were carried out in order to support wind tunnel data and to be compared with a method called CFD testing and validation. These were performed using ANSYS Fluent to complement wind tunnel testing and provide detailed aerodynamic analysis of the blended wing body seaplane design. The flow parameters are assumed to be ISA +13° at 2,400 feet with a flow speed of 51.83 m/s. The simulations focused on evaluating C_l, C_d, C_m, and L/D at α of 3°, 0° and -10° for both the model with and without floats, although this section will only focus on the model with floats, consistent with the wind tunnel experimental conditions. A structured mesh was independently generated, with refined grid regions near the model surfaces to ensure accurate boundary layer resolution and capture flow separation. Flow visualizations, including pressure and velocity contours, were generated to illustrate the aerodynamic performance of both models. These visualizations provided insight into pressure distribution across the wing-body surfaces, wake structures, and flow separation regions, highlighting the aerodynamic penalties introduced by the floats.

V. Results

A. Float Drag Study

The drag forces acting on the floats is summarized in Figure 6.

	Type I	Type II	Type III
Force [kN]	21.7	21.9	19.6

Fig. 6 Drag Forces on Float Designs

From Figure 6, it can be seen that the third design configuration has the lowest drag magnitude when compared to the other two designs by about 11%. Therefore, the Type III design should be the design used in the seaplane model. The velocity contours along the plane of symmetry are shown in Figure 7.

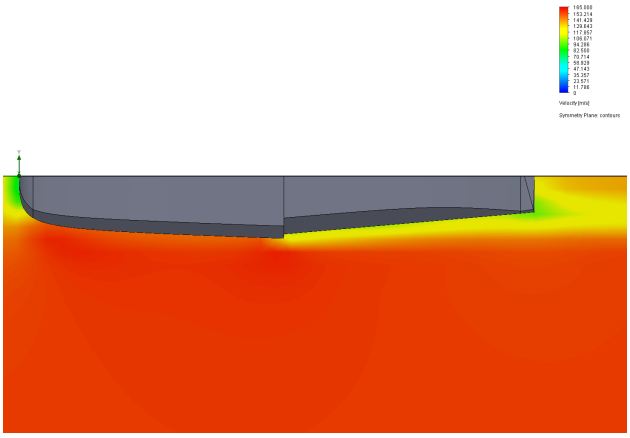

Fig. 7 Float Type III Velocity along Symmetry Plane

B. Wind Tunnel Testing

From the wind tunnel testing, it is evident that the floats caused a penalty in the desirable aerodynamic properties of the aircraft. It is shown in Figure 8 that the lift coefficient magnitude of the no floats model is noticeably greater for the tested range, also showcasing a larger lift slope.

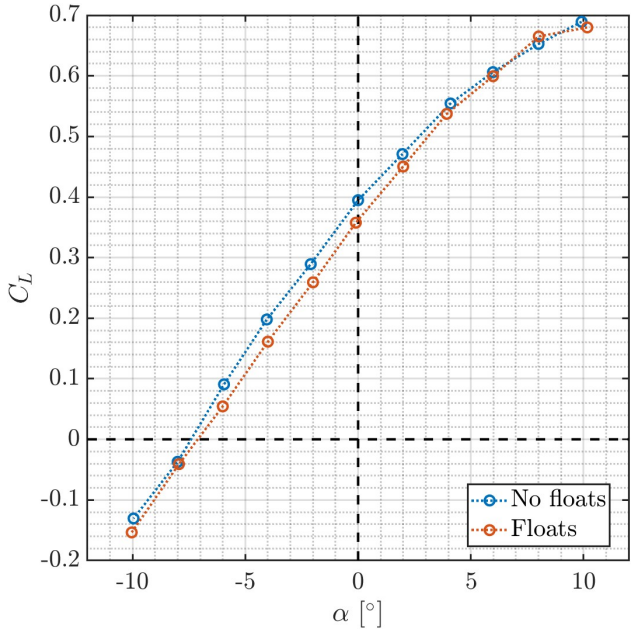

Fig. 8 C_l vs. α for no floats and floats-equipped models

The drag penalty caused by the floats can similarly be seen in Figure 9, although the drag data for the no floats model has unexpected fluctuations not present in the floats model, which can explain the difference in the shape of the plots. The drag coefficient was generally larger for the floats model, which is not evident at first glance due to the irregularities in the no floats data points, as mentioned previously. The drag results confirm that floats introduce a noticeable penalty, as predicted.

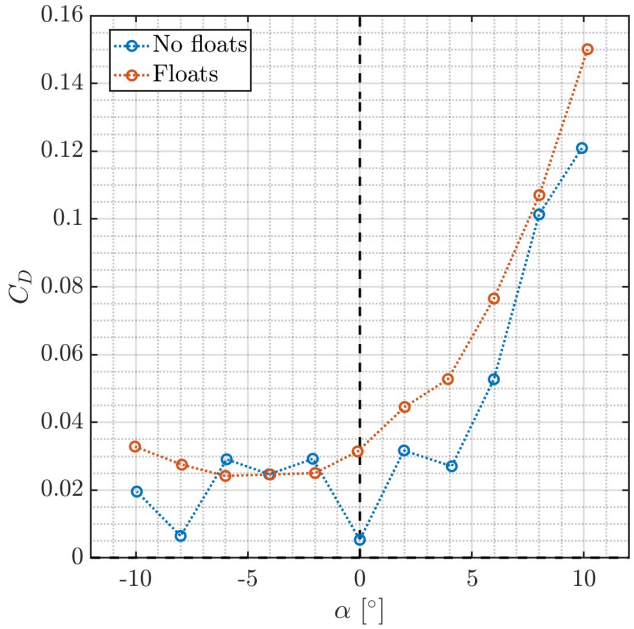

Fig. 9 C_d **vs.** α **for no floats and floats-equipped models**

The longitudinal stability of the two models is seen in Figure 10 showcasing the obtained pitching moment coefficient, from which it is clear that both are not longitudinally stable since the slope of both plots as a function of α is positive. It was expected that the aircraft was unstable in pitch, mainly due to the lack of a tail, which causes the model to not have a counterbalancing force.

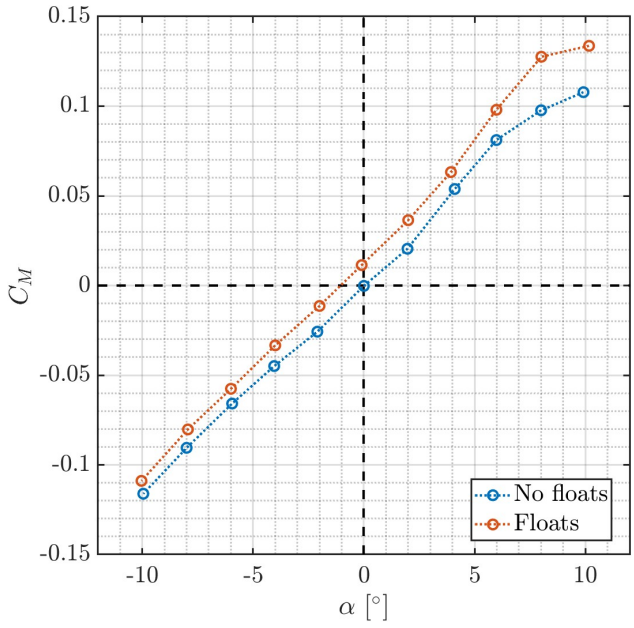

Fig. 10 C_m **vs.** α **for no floats and floats-equipped models**

The lift-to-drag ratio comparison shown in Figure 11 represents the difference in aerodynamic performance between the two models by comparing them directly, in which it is found that L/D for the no floats model is generally larger than for the float-equipped model, as expected from Figure 11 and Figure 12 showing the lift and drag comparisons, respectively. As in Figure 12, possibly faulty points are present, particularly at $\alpha = 0°$ for the no floats model, so Figure 12 better represents the differences in L/D trend.

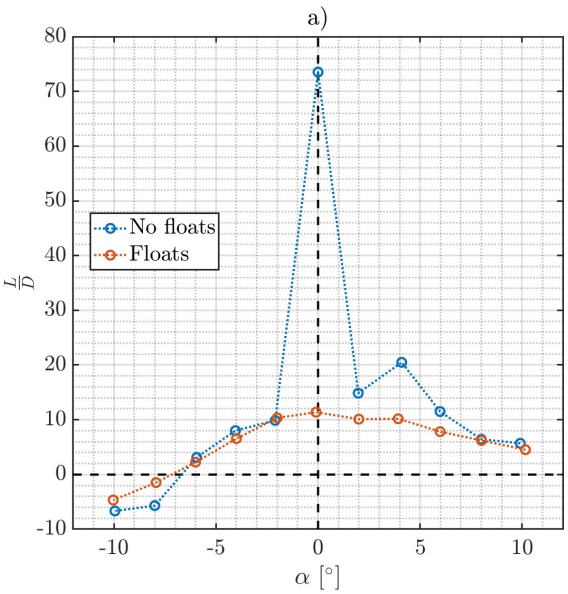

Fig. 11 L/D vs. α for no floats and floats-equipped models, full data set

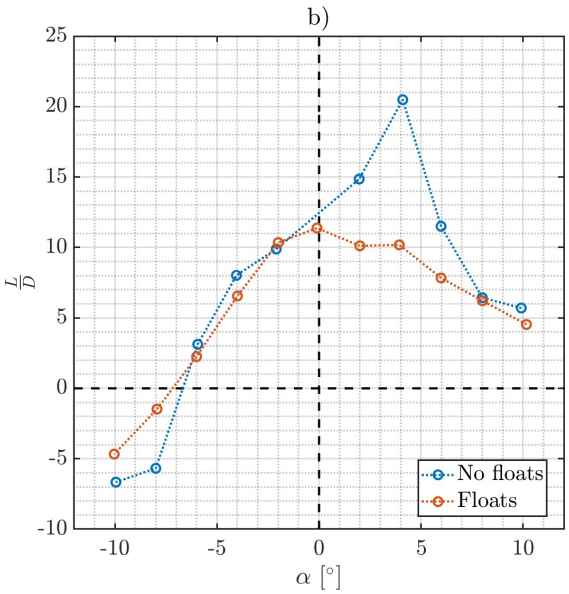

Fig. 12 L/D vs. α for no floats and floats-equipped models, omitting faulty data point

C. Computational Fluid Dynamics Results

1. Drag Penalty Results

The aerodynamic efficiency of the configuration is severely impacted by the addition of floats. Without floats, the L/D is calculated at 486.41, indicating an extremely efficient design with minimal drag. However, when floats are incorporated, the L/D plummets to 9.74. This reduction by a factor of approximately 50 shows that the floats introduce a substantial drag penalty, as expected. The increased drag arises from additional surface area and flow disturbances associated with the floats. Such a drastic decrease in the L/D implies that operational performance metrics will be significantly compromised when floats are used.

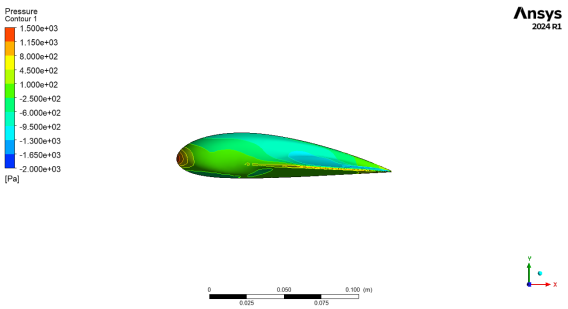

Fig. 13 Pressure contours for scaled down model without floats, sideview

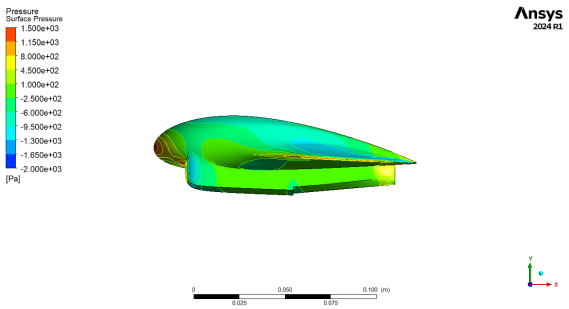

Fig. 14 Pressure contours for scaled down model with floats, sideview

The models above exhibit smooth pressure distribution, with high-pressure regions concentrated at the leading edge of the wing and fuselage nose due to stagnation effects. The addition of floats introduces localized high-pressure zones at the float leading edges and attachment points, increasing drag. Additionally, the low-pressure regions behind the floats contribute to flow separation and wake expansion, leading to an overall increase in aerodynamic drag. The pressure distributions over the wing remain similar.

2. CFD Validation

It is observable from the CFD results that the floats decrease the lift exhibited by the plane, which is also observable from the wind tunnel results. It is shown in Figure 15 that there is a significant difference in the C_l between the two models.

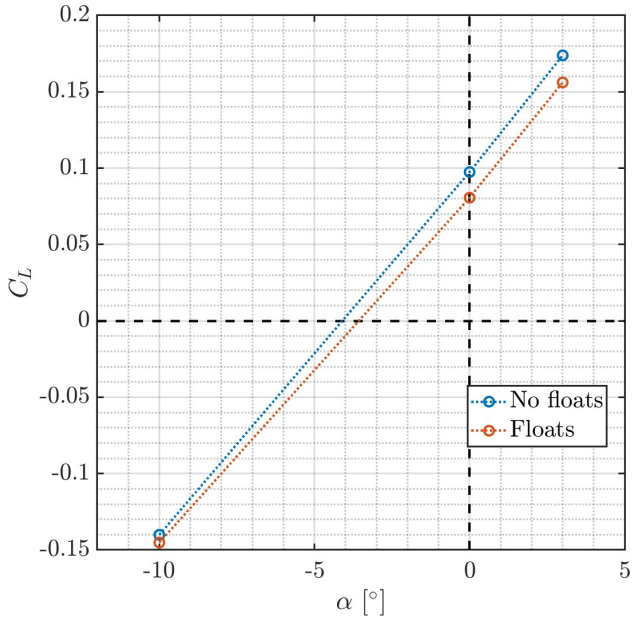

Fig. 15 C_l vs. α for no floats and floats-equipped CFD models

The drag penalty added by the floats can be clearly seen in Figure 16, just as in the wind tunnel results. A similar relationship also exists, where the drag decreases slightly before increasing again as the α goes from negative to positive.

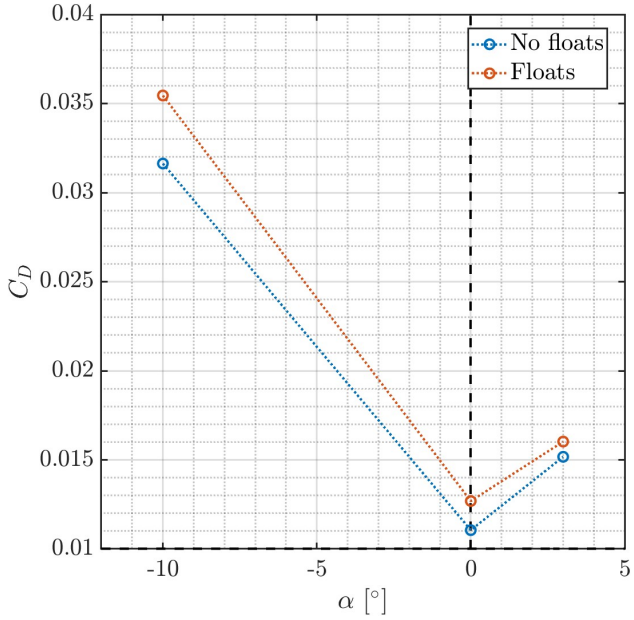

Fig. 16 C_d vs. α for no floats and floats-equipped CFD models

The data shown in Figure 17 shows the pitching moment, which is confirmed to be statically unstable. Unlike the wind tunnel data, the CFD data shows that the no floats model has a higher C_m than the floats model. However, the pitching moments are close to each other, and overall the inclusion of floats does not significantly affect the pitching moment.

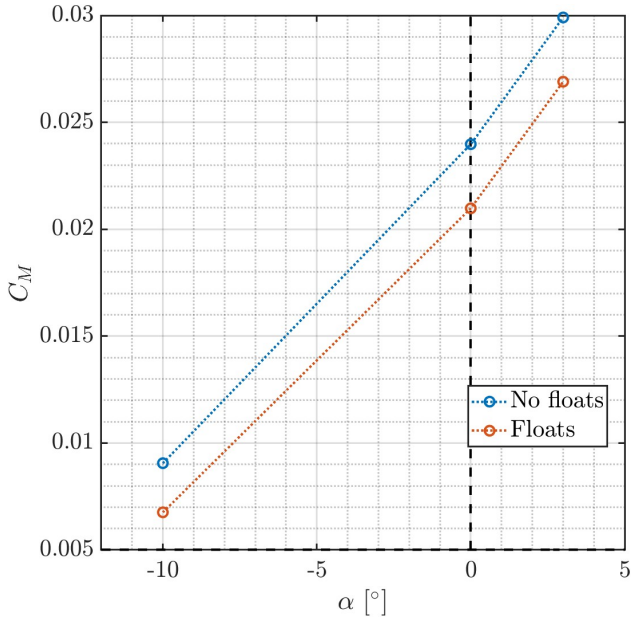

Fig. 17 C_m **vs.** α **for no floats and floats-equipped CFD models**

Figure 18 shows the L/D of the two models. The CFD data shows that the data point at $\alpha = 0°$ was a data error and is right to be excluded. The L/D ratio is higher for the model without floats, which is as expected since the floats both increase drag and decrease lift.

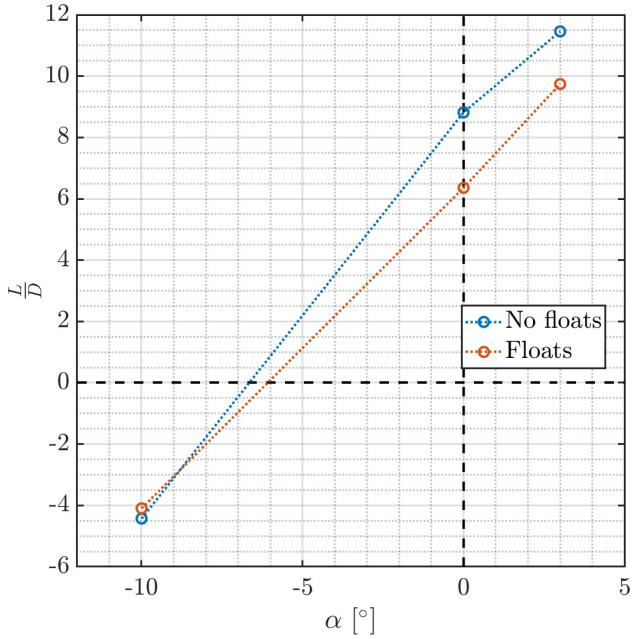

Fig. 18 L/D **vs.** α **for no floats and floats-equipped CFD models**

There is some data mismatch between the CFD results and the wind tunnel results. This is likely due to errors with the wind tunnel, as the wind tunnel was run at maximum settings and the tunnel is not typically calibrated well at that level. Additionally, the wind tunnel models are large, so the possibility of blockage effects and wall interferences is very high, and the surface roughness is higher compared to the ideal surface roughness used in the CFD simulations. The compounding of these errors is what leads to a 2.5 to 3 times difference in resultant data.

VI. Future Plans

Our next steps for this project include testing two different test conditions: test condition 1 which will be a cruising condition (ISA + 15℃ at 10,000 feet and V = 300 knots) with an angle of attack range from -8° to +8°, and test condition 2 which will be a sea level condition (ISA + 15℃ at sea level and V = 110 knots) with an angle of attack range from -8° to +15°. The results of CFD analysis conducted at these conditions will give better design parameters to use for the second iteration of the seaplane. This new design will incorporate new airfoils for the fuselage and wing, as well as an added vertical tail. Design point parameters, such as wing area and wing span, will also be updated through the sizing calculations using the results of the CFD analysis. Additionally, design iterations will be created for different engine placement options. Talks are in progress with the University of Arizona AeroLab to utilize the Arizona Low-Speed Wind Tunnel (ALSWT). Using the ALSWT would enable a larger model to be used, thus providing a more accurate picture of the results. CFD Validation of the results would also be conducted.

VII. Conclusion

This study evaluated the aerodynamic performance of a blended wing body seaplane for offshore missions using both wind tunnel testing and CFD simulations. The no floats configuration exhibited excellent efficiency; however, the addition of catamaran-style floats imposed a severe drag penalty. These results underscored the critical need for design refinements, particularly in float geometry and overall configuration, to mitigate drag and enhance stability. Future work will focus on optimizing these parameters to fully realize the potential of the BWB seaplane concept.

Acknowledgments

The authors would like to express sincere gratitude to Charles Simpson and the New Nose Company for the generous support, resources and expertise that significantly contributed to the Blended Wing Body Seaplane project. We would also like to thank the Aerospace and Systems Engineering Department at the University of Arizona for their continuous support throughout this research. Special thanks to Professor Doug May for his invaluable guidance and mentorship. The authors also extend appreciation to the AIAA student chapter for providing resources and encouragement.

References

[1] Jackson, P., *Jane's All the World's Aircraft 2011–2012*, IHS Jane's, Coulsdon, U.K., 2011.

[2] Roskam, J., *Airplane Design, Part I: Preliminary Sizing of Airplanes*, DARcorporation, Lawrence, KS, 1985.

[3] Roskam, J., *Airplane Design, Part II: Preliminary Configuration Design and Integration of the Propulsion System*, DARcorporation, Lawrence, KS, 1985.

[4] Kozek, M., and Schirrer, A., *Modeling and Control for a Blended Wing Body Aircraft*, Springer, Cham, Switzerland, 2014.

[5] Dathe, I., and de Leo, M., "Hydrodynamic Characteristics of Seaplanes as Affected by Hull Shape Parameters," *AIAA 89-1540-CP*, AIAA 5th Applied Aerodynamics Conference, Seattle, WA, 1989.